Exogenous factors contributing to Column Bed Heterogeneity Part 1: Consequences of 'Air' Injections in Liquid Chromatography.

Jörgen Samuelsson[1], Torgny Fornstedt[1] and Andrew Shalliker[1, 2]

[1]Department of Engineering and Chemical Sciences, INTERACT, Karlstad University, SE-651 88 Karlstad, Sweden

[2]Australian Centre for Research on Separation Science, School of Science and Health, University of Western Sydney, Parramatta, NSW, Australia

* Corresponding author

Jörgen Samuelsson PhD
Phone + 46 54 - 700 1620
Mobile + 46 73 932 81 69
Fax +46 54-700 2040
Email: Jorgen.Samuelsson@kau.se

Abstract

It has been shown that not only the packing homogeneity, but also factors external to the column bed, such as, frits and distributors can have important effects on the column performance. This current communication is the first in a series focusing on the impact of exogenous factors on the column bed heterogeneity. This study is based on several observations by us and others that chromatographic runs often, for technical reasons, include more or less portions of air in the injections. It is therefore extremely important to find out the impact of air on the column performance, the reliability of the results derived from analyses where air was injected, and the effect on the column homogeneity. We used a photographic approach for visualizing the air transport phenomena, and found that the air transport through the column is comprised of many different types of transport phenomena, such as laminal flow, viscous fingering like flows, channels and bulbs, and pulsations. More particularly, the air clouds within the column definitely interact in the adsorption, i.e. mobile phase adsorbed to the column surface is displaced. In addition, irrespective of the type of air transport phenomena, the air does not penetrate the column homogeneously. This process is strongly flow dependent. In this work we study air transport both in an analytical scale and a semi prep column.

Keywords: Column bed heterogeneity; Chromatography; Gas transport; Air Injection

1 Introduction

The heterogeneity of chromatography columns is now well documented [1–13] and it is clear that beds are heterogeneously packed in both the radial and the axial directions [1–14], and that such heterogeneities exist in all forms of Liquid Chromatography (LC) columns, be they low pressure open tubular columns, low to medium pressure (Fast protein liquid chromatography) FPLC columns, or High performance liquid chromatography (HPLC) and Ultra High Performance Liquid Chromatography (UHPLC) columns. Most important is , the radial bed heterogeneity because the variation in the fluid flow velocity across the column radial cross section causes severe distortion of the solute band, resulting in 'bowl' like elution profiles [15]. The development of the Active Flow Technology (AFT) column end fitting [16–19] has shown conclusively that band distortions that result from the heterogeneity in packing density can to a very significant degree be moderated since the flow from these AFT columns is collected from the more uniform radial central region of the column bed, hence effectively eliminating wall effects [13] and other aspects that contribute to radial flow heterogeneity. These fittings offer advantages at HPLC scale columns or prep scale columns, including columns utilised in low pressure environments such as FPLC.

While it is safe to say that column bed heterogeneity arises from the packing process [1–14], it is also clear that exogenous factors can lead to radial heterogeneity in the column bed. We detailed this in earlier studies that showed frits were often a contributing factor [20–22]. In this context it is worth stressing that not only the frit contributes to heterogeneous solute zone, but also dead volumes and sample transport through the injection loop [23–25]. From these earlier works there is little doubt that being able to see inside a chromatography column yields great clarity as to the hydrodynamic transport processes through the fluidised porous bed [12,13,15,20–22]. Usually chromatography is conducted using columns made from stainless steel tubes or other opaque materials, packed with a stationary phase that is also opaque. Being able to see inside these types of columns is therefore very difficult. Nevertheless there are a variety of techniques that enable on-column visualisation even for columns that are made in opaque tubes, for example, Currivan, Connelly and Paull used contactless conductivity detectors to study the uniformity of monolithic beds [26]. Also, columns made from plastic tubes can be placed inside an NMR magnet, and MRI allows for

images of the flow hydrodynamics to be visualised [8–11]. Effectively the internal dimensions of the column can be viewed. The difficulty associated with this process is that complex pulse sequences must be developed, the NMR is an expensive 'detector' and adequate spatial resolution is limited.

Alternatively, a great deal of information can be obtained from columns that are packed in glass tubes [12,13,15,20–22], since high pressure glass tubing suitable for HPLC-type applications is available. If these glass tubes are filled with C18 silica and the mobile phase has the exact same refractive index then the otherwise opaque stationary phase becomes perfectly transparent to the eye. Coloured solutes, or solutes with a different refractive index to the C18 silica can then be injected, and their migration paths can be viewed through the column. Photography can be used to record their transportation [12,13,15,20–22]. Shalliker et al., has used this on-column visualisation process to detail the wall effect [13], transport through frits [21,22] and distributors [20], measure column bed heterogeneity [12], and detail viscous fingering phenomena [15,27–30]. All of which are processes that are difficult, if not impossible to describe without being able to see inside the chromatography column.

In this study we have utilised this matched refractive index on-column visualisation process to detail the transport of air through a chromatography column, i.e., 'air' injections in liquid chromatography. In this situation, air has a different refractive index to the mobile phase, hence, as the air displaces the mobile phase from the stationary phase material the stationary phase then becomes visible and the air transportation can be viewed, much in the manner that the earlier viscous fingering experiments undertaken by Shalliker et al. [27,28] were visualised. A reasonable question to ask oneself is why study air injections? In fact, there are numerous reasons; first and foremost, analysts from time to time accidently undertake air injections, either from partially filling an injection loop with air as the fluid lines are compromised, or if the sample vial volume drops below the required level. Other basic operational mistakes may be made, such as incorrect flushing of a newly inserted sample loop or the like. We wonder whether, for example the anecdotal claims by many who practice liquid chromatography, that the first injection is often erroneous, is in fact a result of 'air-injections'? Other reasons to visualise 'air' injections may be found in chemical processes whereby gases are purged through fluidised porous beds, perhaps for the recovery of fossil fuels, or to study greenhouse gas emissions through a fluidised permafrost in a melting Arctic

environment. Nevertheless, the injection of air inside a chromatography column raises the question as to the whether the homogeneity of the column bed has been exogenously affected by air transport into the column. We address this issue with detailed photographic data following the introduction of air into the column. The aim of this study is to experimentally investigate air transport through a chromatographic column. In this study we will investigate how the air transport is affected by changing: the column inner diameter, flow rate and injection volume. We will also demonstrate the effect of a column void on top of the column has on the air transport.

2 Experimental

2.1 Chromatography columns, mobile phases and reagents

Analytical scale (5 mm, i.d.) HR glass columns were supplied by Pharmacia (Sweden, Uppsala) and a 17 mm i.d. column, was supplied from Omnifit with in-house manufactured endfittings. These columns were packed using an axial compression process consistent with the manufacturer's guidelines. The packing material was Kromasil-100-5-C18 (5 μm d_p) AkzoNobel (Bohus, Sweden). The stationary phase was dispersed in acetone, stirred for 10 minutes, and then ultra-sonicated for a further 10 minutes, prior to being poured into the column blank. Once the stationary phase had settled the column end fitting was applied and the bed compressed. The packed bed height was 6 and 5.8 cm for the 17 mm and 5 mm i.d. column, respectively.

The HPLC mobile phase was a mixture of dichloromethane (DCM) and toluene, purchased from VWR International, in the proportion of 45:55 (DCM:Toluene). This composition had the exact same refractive index as the C18 silica. Flow rates, and sample injection volumes varied and are detailed as appropriate in the text.

2.2 Instrumentation

A Jasco PU 1580 HPLC pump (JASCO, Japan) was used for the delivery of all mobile phases. A Midas auto injector from Spark Holland (AJ Emmen, The Netherlands) was used for sample injection. Detection was achieved photographically using a Nikon D5100 SLR camera (Nikon Corporation, Japan) fitted with a variable focal length 18 to 300 lens (Nikon

Corporation, Japan) fixed at 300 mm for image acquisition. The f-stop was set at 10, and the camera was operated in video record mode. Still photographs were taken as 'snap-shots' from these videos using Adobe Photoshop CS6. In order to minimise the cylindrical lens effect of the tubular column, the column was housed in a standard 30 × 40 × 30 cm tank, which was illuminated using an 8 Watt white fluorescent light tube (Diversa, Poland) located directly behind the HPLC column.

3 Results and Discussion

Once the mobile phase having the same refractive index as the stationary phase has fully equilibrated with the stationary phase, the column and stationary phase become perfectly transparent to the eye, and we have reported this phenomenon on many occasions, and the reader is referred to references [12,13,15,20–22,27–30] for verification of the visual clarity of the technique. When a sample of dye is injected into the column the solute is transported through the bed and its migration path can be visualised, as evidenced by the photographic images reported in these references.

Likewise, migration through a packed bed that displays this 'invisible bed' phenomenon can be visualised if the injection plug has a different refractive index to the mobile and stationary phases. In that case, the injection plug appears as a dark shadow since the light illuminating the bed from behind cannot penetrate the bed. In this study our injection plug was air, which has a different refractive index to that of the C18 silica and hence, the presence of air inside the column can be seen as a shadow as it migrates along the column, since the presence of the air allows the bed itself to be seen. Throughout the course of this study we tested the effects of air injections at various injection volumes, flow rates and column formats (5 and 17 mm i.d.). The results from which are systematically discussed according the observations on 17 mm i.d. and then 5 mm i.d. columns.

3.1 Air Injections on a 17 mm internal diameter column

Typical injection volumes on a 17 mm i.d. column in non-overloaded conditions are around 50 to 300 μL, while in overloaded conditions users would typically inject as much as 2 mL. Hence in this study we tested air injection effects within these limits. In the photographs shown in Fig. 1, a 1000 μL injection of air was made at the flow rate of 2 mL/min. The first

of these photographs (1a) shows the bed prior to the air reaching the column, while photograph 1b shows the appearance of the air 40 seconds after injection, then 1c, 60 seconds after injection. The series of photographs that follow show the propagation of the air plug as it migrates through the column, each photograph recorded 20 seconds apart. When the air initially enters the column the entire column radial cross section is penetrated. However, as time passes the air migrates towards the column radial central zone forming a cone. Shortly thereafter the leading edge of the cone splits and two major regions of the air band migrate along the column. These channels remain saturated with air for the entire length of the column. At the trailing edge of the air injection plug the air slowly dissolves in the incoming mobile phase, but at a rate that is slow relative to the overall migration time. The total time required for all air to leave the column was in this instance 405 seconds; this is around 2 column volumes assuming a porosity of 0.7.

When the injection plug volume was decreased the severity of the effects of the air were naturally also decreased. The photographs in Fig. 2 for example, detail air injections when the plug volume was 500 μL, also at the flow rate of 2 mL/min. The first of these photographs recorded at 20 seconds shows the bed prior to the air injection, thereafter, the photographs show the propagation of the air at 10 second intervals, up to photograph (2g), then photograph (2h) shows the air injection plug at 210 seconds. Similar to the 1000 μL injection air plug, upon entry to the column the air fully saturates the column radial cross section and then forms a cone as the air is concentrated towards the radial central region of the column. The air penetration depth into the column appears to reach a limit, about 1/3rd the length of the column (at 80 seconds – Fig. (2g)) with dissolution of the air occurring at the inlet side of the plug.. However, upon continued observation a new phenomenon is observed, one that reappeared under a variety of conditions that we will demonstrate later in this text, and that is, the transport of what appeared to have been dissolved air and thus invisible, suddenly is ‘precipitated’ from solution and a cloud of air is then visible migrating along the column throughout the entire length. This is illustrated in Fig. 2h. A variety of cloud formations appeared throughout the air migration process, resembling viscous fingering phenomena, e.g. [15]. The air was finally removed from the column after 360 seconds (around 1.3 column volumes), slightly faster than when a 1000 μL air injection was made.

Air injection effects were less spectacular when the injection volume was reduced to 200 μL. The series of photographs recorded at 20 second intervals in Fig. 3 illustrate the air transport process; air fully penetrates the radial column cross section, but does not penetrate beyond the immediate inlet region of the column (~ 5 mm of bed only). Dissolution of the air occurs by the incoming mobile phase. The time required for the air clearance from the column was 90 seconds or 0.3 column volumes.

So far we have only showed how different injection volumes affect the air transport in a column. To investigate how flow rate affects the column a range of flow rates were then tested for each of these injection volumes, however, we limit our discussion to the tests undertaken using a 500 μL injection plug. In Fig. 4 the 500 μL air injection at 1 mL/min is illustrated. In this instance the air fills the entire column radial cross section, forms a cone, and penetrates to a depth of approximately 1/4 the length of the column. A slow process of dissolution follows before the air finally disappears after 570 seconds or around a column volume. The process of the air transport at 2 mL/min has been discussed above – and illustrated by the photographs in Fig. 2. At 3 mL/min similar effects to those observed at 2 mL/min were apparent; that is, the depth of penetration was limited to around 1/3rd the column length, and after a period of time 'clouds' of air reappeared along the column migrating in a 'viscous fingering' type of flow pattern. At 3 mL/min the clearance time was 210 seconds or around a column volume. The series of photographs in Fig. 5 illustrate the transportation process at 3 mL/min.

3.2 *Air Injections on a 5 mm internal diameter column*

While a range of flow rates were tested for air injections made on the 5 mm i.d. column, our discussion here is limited to observations made at 0.5 mL/min. The injection volumes were 100, 200 and 500 μL. Each of these volumes is larger than a regular injection volume usually used on a 5 mm i.d. column, however, these volumes are not beyond the scope of an accidental air load following the change of a sampling loop, pre-column tubing or connection of a switching valve for example. The latter being particularly important in 2D HPLC where injection volumes are larger and there is the potential for a loop to drain when not directly in the pressure flow stream.

The series of photographs in Fig. 6 show the transport of a 100 μL plug of air through the 5 mm i.d. column at 0.5 mL/min. These photographs show that the air upon entry to the column fully saturates the radial cross section of the bed and then forms a cone as the air migrates towards the radial central region of the bed. After 60 seconds (0.6 column volumes) the air appears to have almost fully dissolved, however, its dissolution was short lived as the air was then precipitated out of solution and a substantial cloud formed that then enlarged upon migration through the column. Upon close inspection of the photographs and the video data recorded, the formation and subsequent propagation of the air cloud appeared to follow a viscous fingering process with very finely detailed finger development. The air required 150 seconds to clear from the column or around 1.5 column volumes.

When the injection volume was increased to 200 μL the effects observed at 100 μL were also apparent, but with greater visual clarity (Fig. 7). Upon entry to the column the air plug fully saturated the radial column cross section, and then formed a cone, and the inlet edge of this cone was slowly dissolved by the incoming mobile phase. Interestingly the leading point of the cone appeared to remain static (Figs. 7b to 7f), but at approximately 80 seconds (around 0.8 column volume) there was a sudden burst of air precipitating from solution in a fashion that resembled the explosion of fireworks – Fig. 7f. This cloud then further developed and enlarged, while at the same time the cone at the column inlet slowly dissolved – see Figs. 7f to 7i. Total clearance time from the column was 175 seconds or around 1.8 column volumes.

At injection volumes of 500 μL the air plug was too large to gain detailed information relating to the transport of the air through the column. Other than to say, the process was similar to that observed when the injection plug was 200 μL: the air initially saturated the entire column radial cross section, a cone developed, the inlet point of this cone slowly dissolved and then a cloud burst of air appeared at the front edge of the air zone – this process is detailed in the photographs shown in Fig. 8. In this instance the air required 235 seconds to clear the column entirely or around 2.4 column volumes.

Finally how void volumes on top of the column inlet affects the air transport was investigated. To investigate this 500 μL air injection was conducted on a column with a small void above the stationary phase. The interesting observation was that some of the air remained in the void and was slowly dissolved by the mobile phase, see Fig. 9, but a portion continued to elute through the bed in processes described above, including the process of

precipitation, which resulted in clouds of air propagating along the column. The reason why air remained between the inlet fitting and the bed head is probably that the surface tension in the air bubble is too large to force all the air into the packed bed. As a consequence some air is trapped in the void space and is dissolved in the mobile phase. This clearly shows that packing heterogeneities, such as, packing densities and voids could severely affect the air transport in the column. In this case introducing voids will drastically reduce the potential effect of air in the column, but it does not remove it entirely. However, from a chromatographic perspective introducing voids will result in a reduction of the column efficiency and is generally not recommended.

3.3 Gas transport phenomena observed in this study

We have shown that air is transported in several different ways in a chromatographic column. Initially if sufficient air is introduced the air will enter the column saturating the entire column radial cross section. This indicates that initially the flow of air entering the bed is more or less lamina, even if the viscosity contrast between the air and mobile phase is large. This observation is in line with classical fluid dynamic experiments studying turbulent flow: Where it takes some distance from the flow source before turbulent flow can be established. After this initial entry phase, air forms a cone shaped profile as it migrates along the column, the reason for this is unclear at this point in time. One explanation could be that the local flow rate is fastest in the central part of the column than at the wall regions resulting in a cone shaped profile. It is clearly apparent that air precipitation occurs at distances substantially in front of the visual moving air band. Once this air precipitation phenomenon occurs, the subsequent transport follows a viscous fingering type of effect. This is perhaps not surprising given the very large difference in viscosity between air and the mobile phase used here. During this transport cloud like formations appeared throughout the air migration process, resembling viscous fingering phenomena.

Inspecting the fine structure of the cloud like structures we could observe that it consist of fine lines connecting small bulbs. Probably there exists fine channels invisible to the naked eye and the camera and the air is transported through these small channels in a soluble state, precipitating when a larger void space is attained (see Fig.10). One other interesting observation that we cannot capture on still photographs is that these new fine channels and bulbs appear in a pulsating fashion. One plausible explanation to this is that it takes some pressure to form these channels. As the air is accumulating in a bulb the local pressure

297 increases and at a critical pressure is pushed through the channel. This simple explanation
298 could also explain why these channels more or less drastically can change direction; because
299 the channels are open in a direction with lowest threshold pressure.
300

301 # 4 Conclusion

302
303 The photographic data we have presented here show some fascinating air transport
304 phenomena, perhaps the most surprising of which is the sudden burst of air clouds from air
305 that had apparently already dissolved, or not adsorbed to the surface, see Figs. 6 and 7. This
306 phenomenon is difficult to illustrate through still images, but is far more apparent when video
307 footage is viewed, or when visualised live in the laboratory. The air transport through the
308 column seems to be a combination of much different type of processes. We have observed;
309 laminal flow, viscous fingering like flows, channels and bulbs, and pulsations.
310 To make things more interesting the air transport process is also strongly dependent on the
311 flow rate. We observed that the air precipitation was largest at 2 mL/min. Fig. 2 compared to
312 both lower (1 mL/min., Fig. 4) and higher flow rate (3 mL/min., Fig. 5). In this study two
313 column diameters were investigated, 5 and 17 mm inner diameter. Some substantial
314 differences were apparent. Firstly, on the wider column the air transport could form several
315 cloud like structures see Fig. 1. In the smaller format only one large cloud like structure was
316 formed. Perhaps, however, this may not be a general case.
317
318 Irrespective of the type of air transport phenomena that occurred, one point is clear; the air
319 does not penetrate the column homogeneously, and most importantly the air displaces mobile
320 phase from within the stationary phase. Undoubtedly this would affect the nature of solute-
321 stationary phase interactions as the solvent environment at the surface is temporarily altered.
322 Hence, following air injection the column must be re-equilibrated to establish 'initial'
323 conditions. How long re-equilibration must be is at this point in time uncertain, but what is
324 clear, is that the air takes a surprisingly long period of time to migrate and clear from the
325 column. Perhaps what we have seen here may be why from time to time chromatographers
326 claim the first injection is never the correct outcome.
327
328 The introduction of small voids on top of the column drastically changed the outcome; some
329 air remained at the top of the column in bubbles and did not penetrate the bed until fully

dissolved. Once dissolved, these air bubbles were transported through the column, but at times, the air precipitated from solution and appeared as cloud bursts at various internal locations deep inside the bed. From a chromatographic perspective, introducing voids will result in a reduction of the column efficiency and is generally not recommended.

Acknowledgements

This work was supported by the Swedish Research Council (VR) in the project "Fundamental studies on molecular interactions aimed at preparative separations and biospecific measurements" (grant number 621-2012-3978) and by the Swedish Knowledge Foundation for the International visiting Professor Andrew Shalliker (grant number 20140028). Dedicated to the memory and mentorship of our esteemed teacher – Distinguished Professor Georges Guiochon.

References

[1] J.H. Knox, G.R. Laird, P.A. Raven, Interaction of radial and axial dispersion in liquid chromatography in relation to the "infinite diameter effect," J. Chromatogr. A. 122 (1976) 129–145.

[2] J.H. Knox, J.F. Parcher, Effect of the column to particle diameter ratio on the dispersion of unsorbed solutes in chromatography, Anal. Chem. 41 (1969) 1599–1606.

[3] C.H. Eon, Comparison of broadening patterns in regular and radially compressed large-diameter columns, J. Chromatogr. A. 149 (1978) 29–42.

[4] J.E. Baur, R.M. Wightman, Microcylinder electrodes as sensitive detectors for high-efficiency, high-speed liquid chromatography, J. Chromatogr. A. 482 (1989) 65–73.

[5] T. Farkas, J.Q. Chambers, G. Guiochon, Column efficiency and radial homogeneity in liquid chromatography, J. Chromatogr. A. 679 (1994) 231–245.

[6] T. Farkas, M.J. Sepaniak, G. Guiochon, Column radial homogeneity in high-performance liquid chromatography, J. Chromatogr. A. 740 (1996) 169–181.

[7] T. Farkas, G. Guiochon, Contribution of the Radial Distribution of the Flow Velocity to Band Broadening in HPLC Columns, Anal. Chem. 69 (1997) 4592–4600.

[8] U. Tallarek, E. Baumeister, K. Albert, E. Bayer, G. Guiochon, NMR imaging of the chromatographic process migration and separation of bands of gadolinium chelates, J. Chromatogr. A. 696 (1995) 1–18.

[9] D. Van Dusschoten, U. Tallarek, T. Scheenen, U.D. Neue, H. Van As, Spatially resolved transport properties in radially compressed bead packings studied by PFG NMR, Mag. Res. Imag. 16 (1998) 703–706.

[10] U. Tallarek, E. Bayer, G. Guiochon, Study of Dispersion in Packed Chromatographic Columns by Pulsed Field Gradient Nuclear Magnetic Resonance, J. Am. Chem. Soc. 120 (1998) 1494–1505.

[11] U. Tallarek, E. Bayer, D. Van Dusschoten, T. Scheenen, H. Van As, G. Guiochon, et al., Dynamic NMR microscopy of chromatographic columns, AIChE J. 44 (1998) 1962–1975.

[12] R.A. Shalliker, V. Wong, B.S. Broyles, G. Guiochon, Visualization of bed compression in an axial compression liquid chromatography column, J. Chromatogr. A. 977 (2002) 213–223.
[13] R.A. Shalliker, B.S. Broyles, G. Guiochon, Physical evidence of two wall effects in liquid chromatography, J. Chromatogr. A. 888 (2000) 1–12.
[14] V. Wong, R.A. Shalliker, G. Guiochon, Evaluation of the Uniformity of Analytical-Size Chromatography Columns Prepared by the Downward Packing of Particulate Slurries, Anal. Chem. 76 (2004) 2601–2608.
[15] H.J. Catchpoole, R.A. Shalliker, G.R. Dennis, G. Guiochon, Visualising the onset of viscous fingering in chromatography columns, J. Chromatogr. A. 1117 (2006) 137–145.
[16] M. Camenzuli, H.J. Ritchie, J.R. Ladine, R.A. Shalliker, Enhanced separation performance using a new column technology: Parallel segmented outlet flow, J. Chromatogr. A. 1232 (2012) 47–51.
[17] M. Camenzuli, H.J. Ritchie, J.R. Ladine, R.A. Shalliker, The design of a new concept chromatography column, Analyst. 136 (2011) 5127–5130.
[18] R.A. Shalliker, M. Camenzuli, L. Pereira, H.J. Ritchie, Parallel segmented flow chromatography columns: Conventional analytical scale column formats presenting as a "virtual" narrow bore column, J. Chromatogr. A. 1262 (2012) 64–69.
[19] M. Camenzuli, H.J. Ritchie, R.A. Shalliker, Improving HPLC separation performance using parallel segmented flow chromatography, Microchem. J. 111 (2013) 3–7.
[20] R.A. Shalliker, B.S. Broyles, G. Guiochon, Visualization of sample introduction in liquid chromatographic columns: Contribution of a flow distributor on the sample band shape, J. Chromatogr. A. 865 (1999) 83–95.
[21] B.S. Broyles, R.A. Shalliker, G. Guiochon, Visualization of sample introduction in liquid chromatography columns: The effect of the frit diameter, J. Chromatogr. A. 855 (1999) 367–382.
[22] B.S. Broyles, R.A. Shalliker, G. Guiochon, Visualization of solute migration in chromatographic columns Influence of the frit porosity, J. Chromatogr. A. 917 (2001) 1–22.
[23] J. Samuelsson, T. Fornstedt, Injection Technique for Generating Accurate Adsorption Isotherm Data Using the Elution by Characteristic Points Method, Anal. Chem. 80 (2008) 7887–7893.
[24] J. Samuelsson, L. Edström, P. Forssén, T. Fornstedt, Injection profiles in liquid chromatography. I. A fundamental investigation, J. Chromatogr. A. 1217 (2010) 4306–4312.
[25] P. Forssén, L. Edström, J. Samuelsson, T. Fornstedt, Injection profiles in liquid chromatography II: Predicting accurate injection-profiles for computer-assisted preparative optimizations, J. Chromatogr. A. 1218 (2011) 5794–5800.
[26] S. Currivan, D. Connolly, B. Paull, Production of novel polymer monolithic columns, with stationary phase gradients, using cyclic olefin co-polymer (COC) optical filters, Analyst. 137 (2012) 2559–2566.
[27] B.S. Broyles, R.A. Shalliker, D.E. Cherrak, G. Guiochon, Visualization of viscous fingering in chromatographic columns, J. Chromatogr. A. 822 (1998) 173–187.
[28] R.. Shalliker, B.. Broyles, G. Guiochon, Visualization of viscous fingering in high-performance liquid chromatographic columns: Influence of the header design, J. Chromatogr. A. 865 (1999) 73–82.
[29] R.A. Shalliker, V. Wong, G. Guiochon, Reproducibility of the finger pattern in viscous fingering, J. Chromatogr. A. 1161 (2007) 121–131.

[30] R.A. Shalliker, H.J. Catchpoole, G.R. Dennis, G. Guiochon, Visualising viscous fingering in chromatography columns: High viscosity solute plug, J. Chromatogr. A. 1142 (2007) 48–55.

Figure captions

Fig. 1: A 1000 μL air injection at a flow rate of 2 mL/min using a column with 17 mm inner diameter. Photographs were taken at (a) 20, (b) 40, (c) 60, (d) 80, (e) 100, (f) 120, (g) 180, and (h) 210 seconds after the injection. System pressure 1 Bar.

Fig. 2: A 500 μL air injection at a flow rate of 2 mL/min using a column with 17 mm inner diameter. Photographs were taken at (a) 20, (b) 30, (c) 40, (d) 50, (e) 60, (f) 70, (g) 80 and (h) 210 seconds after the injection. System pressure 1 Bar.

Fig. 3: A 200 μL air injection at a flow rate of 2 mL/min using a column with 17 mm inner diameter. Photographs were taken at (a) 20, (b) 25, (c) 30, (d) 40, (e) 50 and (f) 60 seconds after the injection. System pressure 1 Bar.

Fig. 4: A 500 μL air injection at a flow rate of 1 mL/min using a column with 17 mm inner diameter. Photographs were taken at (a) 50, (b) 120, (c) 180, (d) 300, (e) 420 and (f) 540 seconds after the injection. System pressure 0.5 Bar.

Fig. 5: A 500 μL air injection at a flow rate of 3 mL/min using a column with 17 mm inner diameter. Photographs were taken at (a) 20, (b) 30, (c) 40, (d) 60, (e) 100 and (f) 140 seconds after the injection. System pressure 1.6 Bar.

Fig. 6: A 100 μL air injection at a flow rate of 0.5 mL/min using a column with 5 mm inner diameter. Photographs were taken at (a) 30, (b) 40, (c) 50, (d) 60, (e) 70, (f) 80, (g) 90, (h) 100 and (i) 110 seconds after the injection. System pressure 0.5 Bar.

Fig. 7: A 500 μL air injection at a flow rate of 0.5 mL/min using a column with 5 mm inner diameter. Photographs were taken at (a) 30, (b) 40, (c) 50, (d) 60, (e) 70, (f) 80, (g) 90, (h) 100 and (i) 110 seconds after the injection. System pressure 0.5 Bar.

Fig. 8: A 100 μL air injection at a flow rate of 0.5 mL/min using a column with 5 mm inner diameter. Photographs were taken at (a) 30, (b) 80, (c) 90, (d) 100, (e) 110 and (f) 140 seconds after the injection. System pressure 0.5 Bar.

Fig. 9: A photograph showing the air bubbles trapped in the void space between the column bed and inlet head fitting. The air injection volume was 500 µL and the flow rate was 3 mL/min using a column with 5 mm inner diameter. System pressure 1.8 Bar.

Fig. 10: Photograph of air transport following a 100 µL injection of air on a 5 mm column at a flow rate of 0.5 mL/min. The photograph shows the bulb and channels that are formed during the air transport through the column. System pressure 0.5 Bar.

Figure 1.

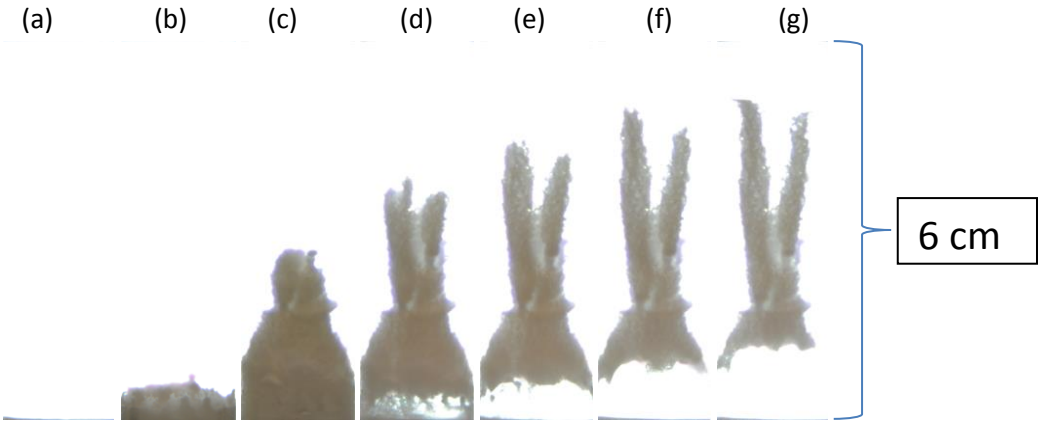

Figure 2

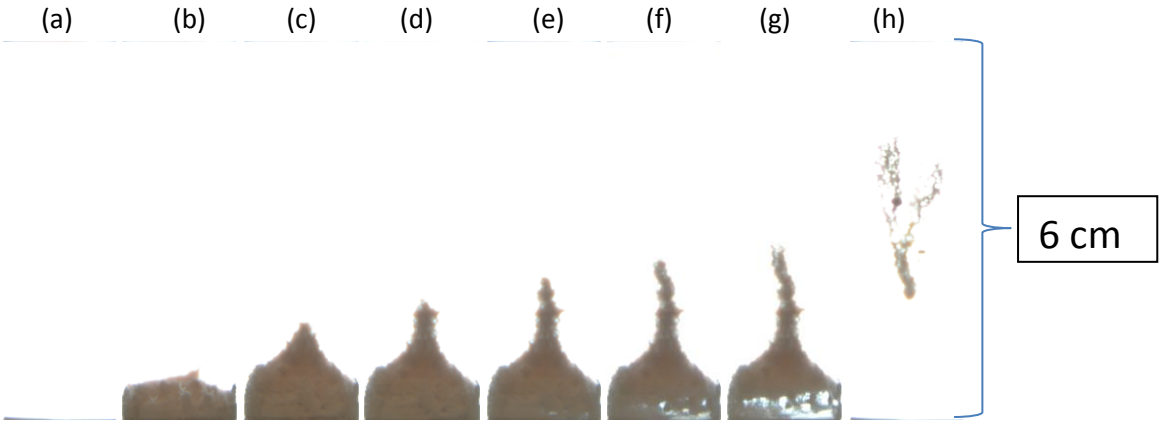

Figure 3

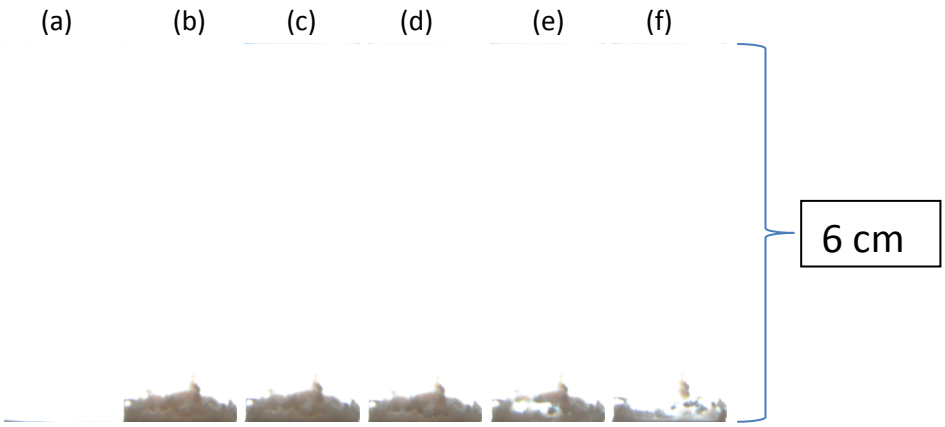

Figure 4

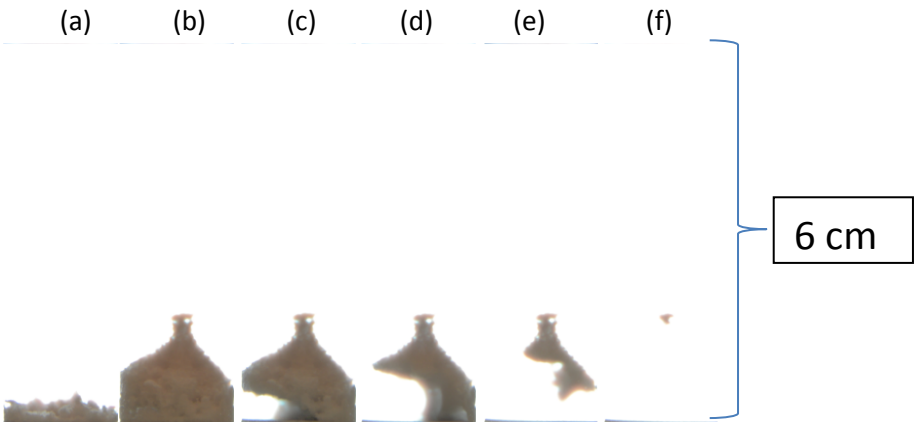

Figure 5

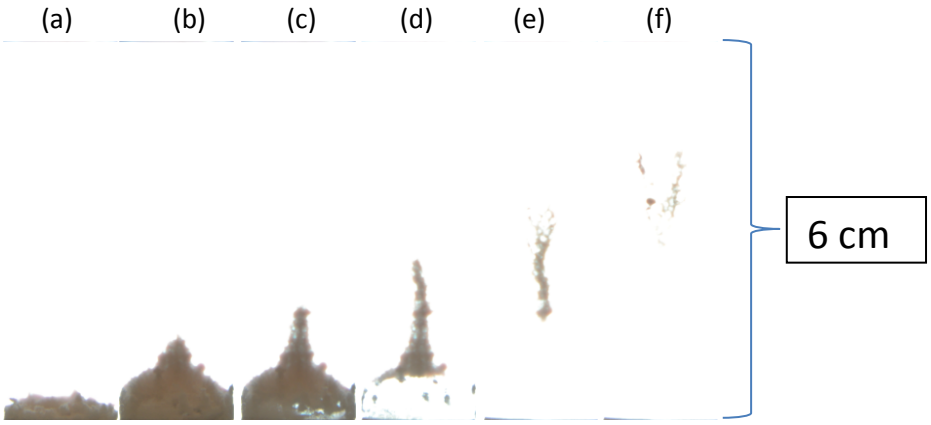

Figure 6

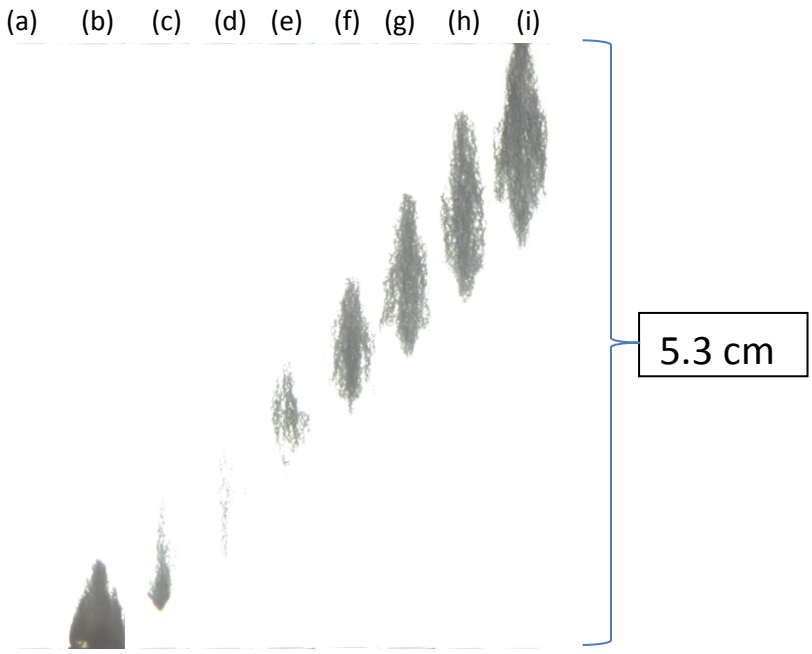

Figure 7

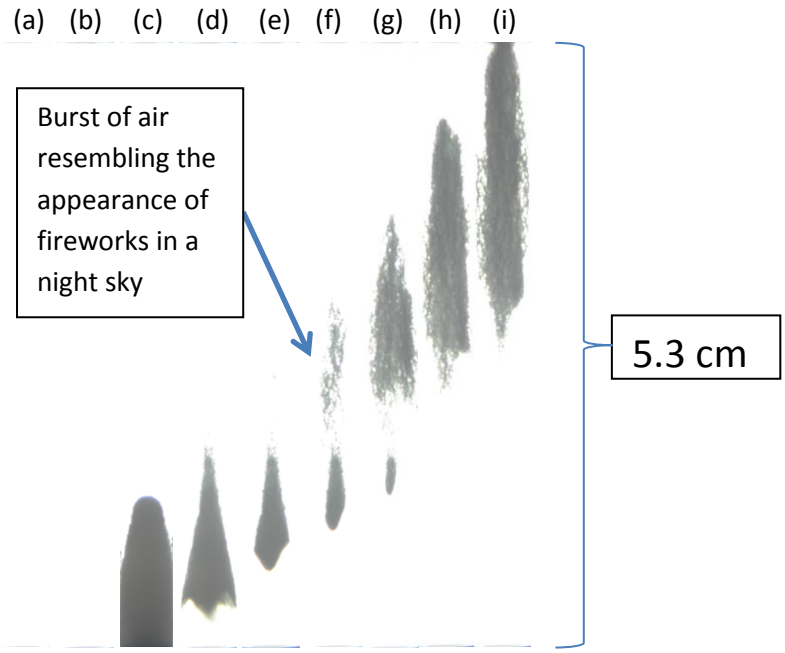
(a) (b) (c) (d) (e) (f) (g) (h) (i)
Burst of air resembling the appearance of fireworks in a night sky
5.3 cm

Figure 8

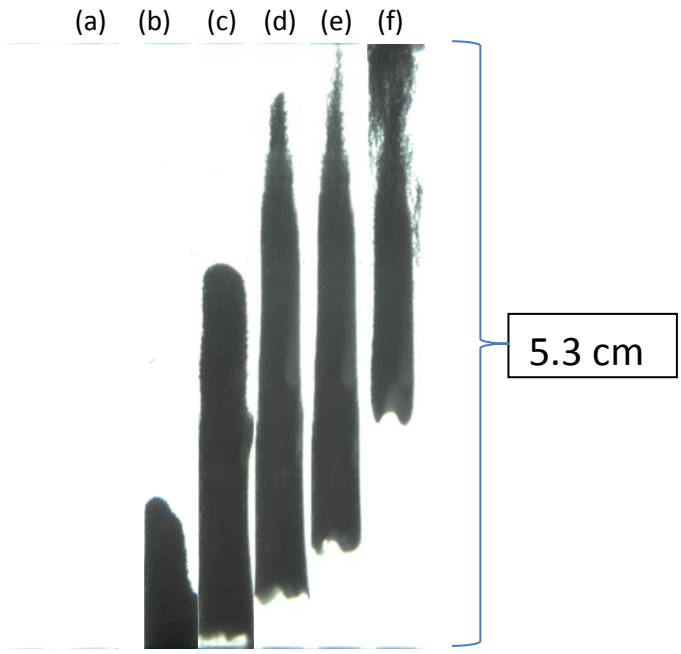

Figure 9.

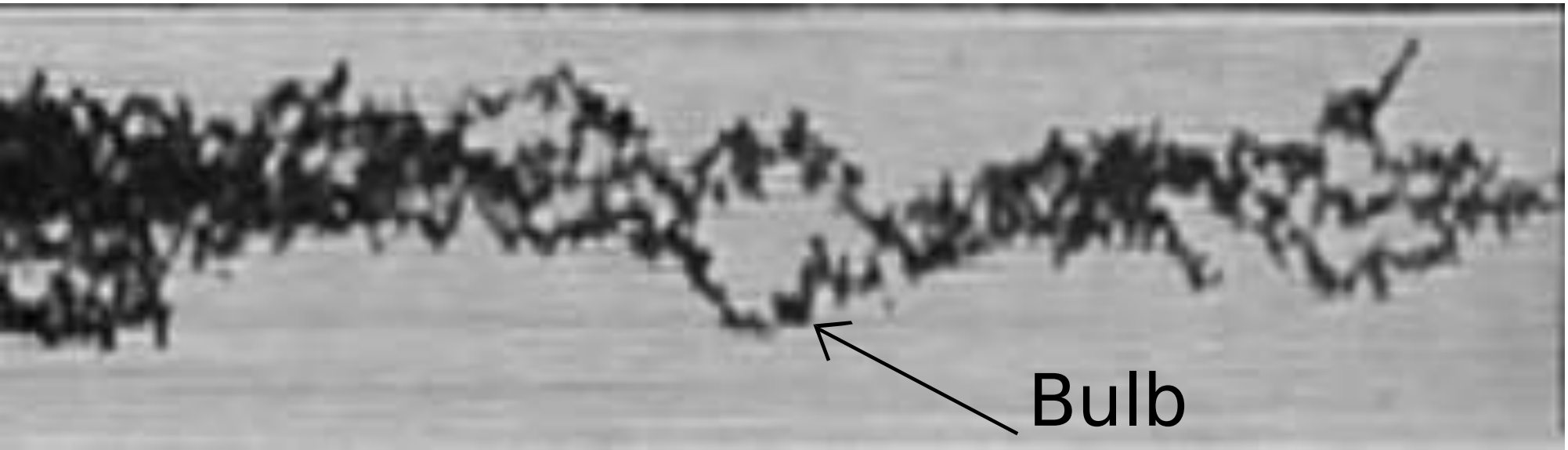
Bulb